Effects of conjoint mechanical and chemical stress on perfluorosulfonic-acid membranes for fuel cells

Mylène Robert, Assma El Kaddouri, Jean-Christophe Perrin, Kevin Mozet, Meriem Daoudi, Jérôme Dillet, Jean-Yves Morel, Stéphane André, Olivier Lottin

Journal of Power Sources 476 (2020) 228662

Contents lists available at ScienceDirect

Journal of Power Sources

journal homepage: www.elsevier.com/locate/jpowsour

Effects of conjoint mechanical and chemical stress on perfluorosulfonic-acid membranes for fuel cells

Mylène Robert *, Assma El Kaddouri, Jean-Christophe Perrin, Kévin Mozet, Meriem Daoudi, Jérôme Dillet, Jean-Yves Morel, Stéphane André, Olivier Lottin

Université de Lorraine, CNRS, LEMTA, F-54000, Nancy, France

HIGHLIGHTS

- A new ex-situ aging device coupling mechanical and chemical stressors was developed.
- Fully hydrated membranes can withstand severe cyclic compression stress.
- Combined chemical and mechanical stresses seem to accelerate membrane degradation.

GRAPHICAL ABSTRACT

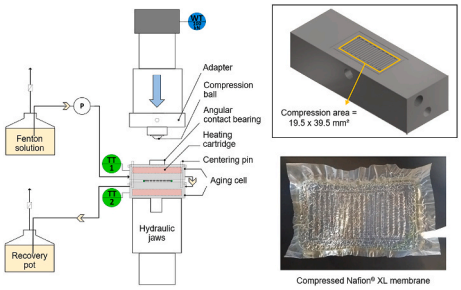

ARTICLE INFO

Keywords:
Chemical degradation
Durability
Fenton's reaction
Nafion® membrane
Mechanical fatigue
PEM fuel Cell

ABSTRACT

To improve the lifetime of proton-exchange membrane (PEM) fuel cells, it is necessary to provide a better understanding of the degradation mechanisms of the perfluorosulfonic acid (PFSA) membranes during fuel cell operation. Despite quantities of work focusing independently on chemical or mechanical degradation, only a few concerned the effect of both combined. The purpose of this study is to analyze the effects of conjoint chemical and mechanical stress on PFSA membranes via an *ex-situ* approach. First, an investigation of the effects of chemical degradation by radical attacks (i.e. exposure to Fenton reagents) on PFSA membranes was carried out. The results confirm that the chemical decomposition of PFSA membranes is significantly influenced by the concentration of Fenton's reagents, both chemically and morphologically. Second, a custom-made device was developed to examine the impact of coupled chemical and mechanical degradations. The initial results show that fully hydrated membranes seem to withstand severe sinusoidal constraints as no crack formed. However, the application of cyclic compression resulted in accelerated chemical decomposition of PFSA membranes. The results also demonstrate that some microstructural changes can appear and lead to a slight increase in the hydrogen crossover that can be detected before it impacts the cell performances.

* Corresponding author.
E-mail addresses: mylene.robert@univ-lorraine.fr (M. Robert), assma.el-kaddouri@univ-lorraine.fr (A. El Kaddouri), jean-christophe.perrin@univ-lorraine.fr (J.-C. Perrin), kevin.mozet@univ-lorraine.fr (K. Mozet), meriem.daoudi@univ-lorraine.fr (M. Daoudi), jerome.dillet@univ-lorraine.fr (J. Dillet), jean-yves.morel@univ-lorraine.fr (J.-Y. Morel), stephane.andre@univ-lorraine.fr (S. André), olivier.lottin@univ-lorraine.fr (O. Lottin).

https://doi.org/10.1016/j.jpowsour.2020.228662
Received 17 April 2020; Received in revised form 8 July 2020; Accepted 12 July 2020
Available online 13 August 2020

1. Introduction

The degradation of perfluorosulfonic acid (PFSA) membranes remains one of the main factors limiting proton-exchange membrane (PEM) fuel cells lifetime, as well as their widespread commercialization [1–4]. During fuel cell operation, PEMs are exposed to harsh conditions, among which aggressive chemical environment and mechanical fatigue prevail. This can alter the membrane properties and lead to performance losses or, in the worst cases, fuel cell shutdown due to membrane failure.

Mechanical fatigue arises mainly from swelling/shrinkage cycles caused by the membrane water-uptake. When repeated many times, these variations in water content weaken the membrane, alter its structure by causing irreversible plastic deformations and may subsequently lead to the formation and growth of cracks and pinholes [5–7]. In addition, despite of the presence of gas diffusion layers on both sides of the membrane-electrodes assembly (MEA), the distribution of constraints remains non-uniform due to the complex shape of the flow field plates.

Chemical damages are primarily due to radical attacks on the most vulnerable sites of PFSA, leading to the scission of the polymer chains (backbone or/and side chains) [8,9] and finally to the thinning of the membrane [10,11]. The aggressive radical environment encountered during fuel cell operation results mostly from reactants crossover through the membrane and the subsequent parasitic electrochemical reactions that entail the formation of hydrogen peroxide and thus free radicals [9,12–15].

Over the past decades, efforts have been made to reduce the ionic resistivity of the membrane without compromising its mechanical robustness. For instance, the Nafion® XL is a PFSA based membrane containing an additional microporous PTFE-rich (PolyTetraFluoroEthylene) layer in its center to provide better mechanical stability and extended lifetime [16]. The central reinforcement layer is impregnated with PFSA on both sides to ensure a continuous conductive pathway through the membrane and enable the use of thinner material. The nominal thicknesses of each layer are about ~12 μm for the PTFE layer and ~9 μm for each external PFSA layer [17,18]. Moreover, Nafion® XL also contains cerium-based chemical stabilizers to mitigate chemical attacks and thus improve its durability [19–21]. Nevertheless, despite their enhanced features, composite membranes remain impacted by chemical attacks during fuel cell operation [22,23].

To better understand the mechanisms of membrane degradation, it is important to discriminate between the effects of chemical and mechanical stressors considered alone and together. Indeed, a few studies have already demonstrated the existence of a synergy between them leading to an acceleration of the membrane decomposition [24–27].

Fenton's reaction is by far the most used *ex-situ* method to study the chemical degradation of PFSA membranes. This reaction of hydrogen peroxide with ferrous ions forms hydroxyl ($HO^{\bullet}$) and hydroperoxyl ($HOO^{\bullet}$) radicals, which have also been observed during fuel cell operation [28]. The recent work of Frensch et al. provided a better understanding of the effect of Fenton's reagents on PFSA membranes by highlighting the high dependence of fluoride emissions on iron and hydrogen peroxide concentrations [29]. Moreover, the authors confirmed that hydrogen peroxide acts as a necessary precursor to form free radicals and that ferrous ions only play the role of catalyst.

Degradation protocols based on Fenton's reaction consist in immersing membrane samples in an aqueous solution of hydrogen peroxide containing traces of ferrous ions to initiate radical attacks. The temperature of the solution is of the order of 80 °C. This method allows an initial assessment of the durability of the membranes even if the rate of chemical degradation achieved is higher than in a fuel cell. However, there is still a need to implement more elaborate ex-situ protocols combining mechanical stress with chemical radical attacks to get closer to fuel cell operating conditions. Recently, specific accelerated stress tests (ASTs) were developed to study the impact of coupled mechanical and chemical stressors on PFSA membranes during fuel cell operation [26,30,31]. For instance, Lim et al. evaluated the *in-situ* degradation of PFSA membranes during conjoint mechanical and chemical membrane accelerated stress tests [30]. They demonstrated that the combination of steady-state Open Circuit Voltage (OCV) phases and periodic wet/dry cycles led to a consistent and fast degradation with significant fluorine losses and uniform membrane thinning. Moreover, they highlighted the acceleration of the overall degradation since membrane failure occurred after only 160 h of operation. Using an *ex-situ* approach, Kusoglu et al. developed a specific compression apparatus in order to study the effect of a normal stress on Nafion® membranes exposed to radical attacks [25]. The authors showed that applying a static compression to a membrane exchanged with ferrous ions and immersed in hydrogen peroxide solution affects its microstructure and accelerates the chemical decomposition of the polymer chains. Nevertheless, to the best of our knowledge, this approach was only carried out by this group. It would therefore be interesting to continue this type of combined experiment by considering conditions more representative of fuel cell operation, such as repeated compression cycles.

Our work aims at exploring the consequences of chemical and mechanical degradations on the morphology and physicochemical properties of Nafion® membranes: chemical structure, as well as water transport and sorption. For this purpose, a specific custom-made device able to mimic chemical and mechanical conditions representative of fuel cell operation was developed. The membrane degradation was induced by exposing the membrane simultaneously to a free radical environment and a cyclic compression. The free radical environment was generated by the circulation of a continuous flow of hydrogen peroxide or Fenton's solution (i.e. hydrogen peroxide and ferrous ions), while the repetition of a 0.1 Hz compression sequence was implemented to induce a mechanical fatigue close to that resulting from the swelling/shrinkage of the membrane during transient fuel cell operation. As a first step, we had to determine the concentration of Fenton's reagents leading to the maximum fluoride emissions – and thus membrane degradation – without inducing extreme morphological changes such as delamination and/or formation of bubbles. Indeed, such phenomena are not observed or at least reported during or after fuel cell operation. In addition, this preliminary study was necessary because there is no consensus in the literature on this matter [11,25,32,33].

2. Experimental

2.1. Materials

2.1.1. Perfluorosulfonated membranes

Nafion® XL and Nafion® NR211 membranes were purchased in the protonated (H^+) form from Ion Power Inc. Both membranes are based on chemically stabilized copolymer of tetrafluoroethylene (TFE) and perfluoro(4-methyl-3,6-dioxa-7-octene-1-sulfonyl fluoride) [34], have similar Ion Exchange Capacity (IEC) – 0.92 meq.g^{-1} for XL and 0.98 meq.g^{-1} for NR211 – and similar nominal thickness – 27.5 μm versus 25.4 μm. Nafion® NR211 is unreinforced while Nafion® XL is a reinforced membrane containing an additional microporous PTFE-rich layer and cerium-based chemical stabilizers.

2.1.2. Membrane preparation

Prior to each utilization, the membrane samples were pretreated according to a procedure close to the one established by Xu et al. [35]: they were first boiled 1 h in 3 wt% hydrogen peroxide solution and rinsed thoroughly with distilled water to eliminate any organic impurities. They were then soaked 30 min at room temperature in nitric acid (10 mol L^{-1}) and boiled 1 h in deionized water. To ensure a complete substitution of the ionomer active sites, the samples were then boiled 1 h in sulfuric acid (1 mol L^{-1}), and 1 h again in deionized water. Finally, they were dried 24 h in an oven at 60 °C.

2.2. Accelerated aging protocols

2.2.1. Ex-situ chemical degradation by Fenton's reaction

The chemical degradation protocol was based on the Fenton's reaction [36] which consists in the reaction between ferrous ion (Fe^{2+}) and hydrogen peroxide (H_2O_2) to form hydroxyl ($HO^{\bullet}$) and hydroperoxyl ($HOO^{\bullet}$) radicals. Various Fenton's solutions were prepared from a 50 mg L^{-1} stock solution of ferrous iron (II) and 30 vol% hydrogen peroxide, provided by VWR Chemicals. The stock solution was first prepared from iron (II) heptahydrate ($FeSO_4.7H_2O$), purchased from Jeulin, and a few drops of concentrated nitric acid were added to lower the pH < 3 before the addition of hydrogen peroxide.

The (24 cm^2) samples were kept completely flat inside the solution thanks to a polycarbonate frame and nylon screws in order to uniformly expose the membrane. The membranes were first cut to size, set in the polycarbonate frame and immersed in a 250 cm^3 beaker (Fig. 1). Membrane degradation was performed during 24 h at 80 °C under magnetic stirring. A watch glass was placed at the top of the beaker to limit water evaporation.

After the test, the samples were rinsed with distilled water before being treated to eliminate cationic contaminant due to iron from Fenton's solution. Membrane's samples were soaked in a EDTA-Na_2 (0.01 mol L^{-1}) complexing solution at room temperature overnight and then boiled in a nitric acid solution (1 mol L^{-1}) at 80 °C during 2 h for re-acidification. Finally, the samples were washed 2 h in distilled water at 80 °C and dried 6 h in an oven at 60 °C prior to any analysis. Moreover, Fenton's solutions were stored before being analyzed to determine the fluorine ion concentration.

2.2.2. Ex-situ coupled mechanical and chemical tests

The combined mechanical and chemical tests were carried out using a custom-made device that mimics the operating conditions of the fuel cell (Fig. 2a). For this purpose, two symmetric half-cells were machined in 316L stainless steel, with single serpentine flow channels (19 passes) similar to those used in fuel cells to ensure the distribution of the solution on each side of the membrane. The land and channels are 1 mm wide and 0.7 mm deep (Fig. 2b).

To induce the chemical degradation, a continuous flow of solution (i.e. H_2O_2 only or Fenton's solution) circulated through the two half-cells between two storage tanks with a flow rate of 3 mL min^{-1} ensuring a residence time of about 10 s per half-cell. An EPDM (Ethylene Propylene Diene Monomer) O-ring gasket was added to ensure perfect sealing. Cartridge heaters and thermocouples were inserted into each half-cell as close as possible to the membrane to maintain the desired temperature (80 °C). This system can accommodate membrane samples 40–45 mm in width and 60–70 mm in length. The area exposed to the solution flow (including the channel ribs) is 19.5 × 39.5 mm^2.

The half-cells were inserted between the clamps of an electromechanical universal testing machine (MTS load frame model 312.21). The mechanical stress was induced through the channel ribs by applying sinusoidal constraints between 0 and 5 MPa at 0.1 Hz during several hours. A preliminary test was carried out to determine the minimal pressure required to compress the gasket and thus ensure an optimum sealing. This minimal pressure was assumed to correspond to the 0 MPa reference seen by the membrane.

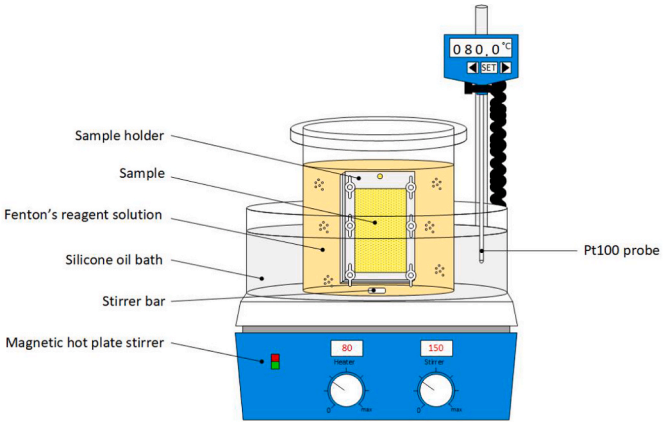

Fig. 1. Schematic representation of the ex-situ chemical degradation setup.

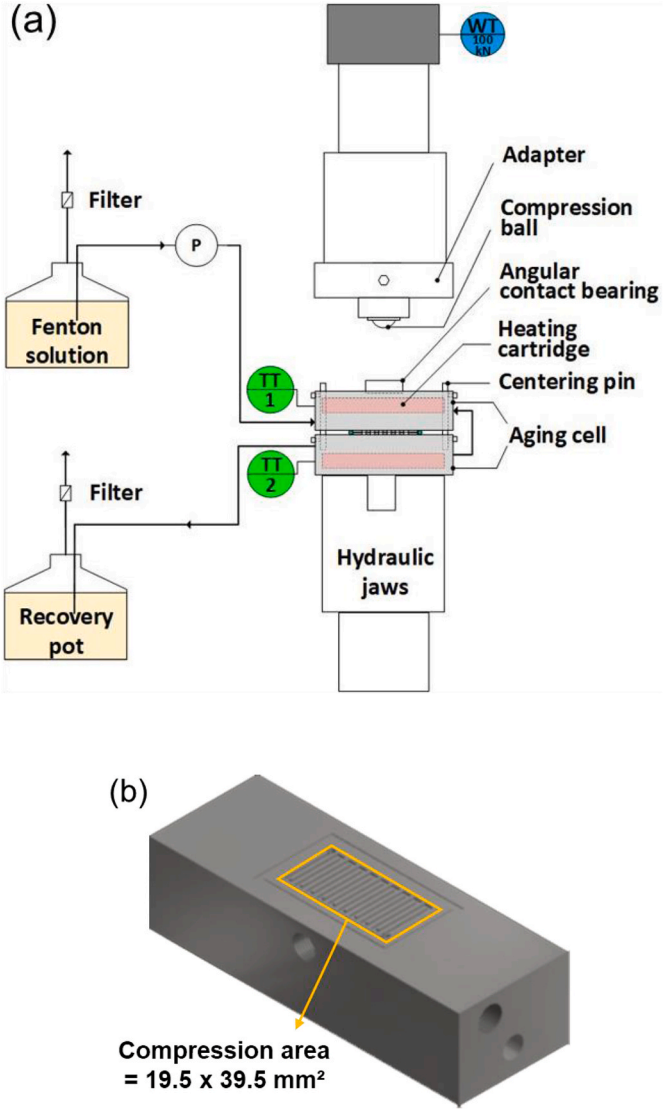

Fig. 2. Schematic representations of (a) the coupled mechanical and chemical degradations device and (b) the lower part of the aging cell designed for this study.

After the tests, the samples were extracted from the cell, immersed in distilled water before being treated with the same complexation/re-acidification protocol than described earlier for ex-situ chemical degradation tests. Membrane samples were finally dried in an oven during 6 h at 60 °C prior to analyses. In addition, the solutions that circulated through the cell were collected and stored before being analyzed to determine the fluorine ion concentration.

2.3. Fluoride emission rate

After each test, the concentration of fluorine ions in the Fenton's solutions and circulating solutions was measured thanks to a pH/millivolt meter (SevenCompact S220, Mettler Toledo) equipped with a fluoride ion-selective electrode (DX219, Mettler Toledo). The

calibration curves ranged from 0.003 mM to 1 mM. The total amount of fluoride released during the degradation experiment was determined from the measured fluoride concentration and the volume of solution remaining after the degradation experiments.

2.4. Electrochemical tests in single cell

Membrane samples submitted to either *ex-situ* chemical stress test or combined mechanical and chemical test were then used to make Membrane Electrodes Assemblies (MEA) to assess their functional properties. The MEA were made according to the following protocol:

- The membranes were inserted between two 235 μm Ga Diffusion Electrodes (GDE) from Hyplat made from Sigracet SGL 29BCE gas diffusion layers with a micro-porous layer. The GDE dimensions were 19 × 38 mm^2 and their Pt loading was 0.3 mg cm^{-2} on a Vulcan carbon. The two GDE were carefully aligned on both sides of the membrane thanks to a set of aluminum plates containing a 100 μm PTFE frame to the GDE dimensions.
- The membrane and GDE were then slightly pressed with a very low force (~50 N) while being heated during 8 min to a temperature of 135 °C.
- After the heating stage, the membrane and GDE were hot pressed 3 min and 30 s with a pressure of 4.1 MPa (3000 N). The temperature of the plates was kept to 135 °C.
- Then, the whole MEA was cooled to ambient temperature.

The MEA were tested in a single cell made of identical gold-coated brass plates on both the anode and cathode sides, with a single serpentine channel (19 passes) of 0.7 mm depth and 1 mm width. The width of the channel rib was 1 mm. The anode and cathode flow field plates were thus similar to those used with the compression device. They were assembled using four M6 bolts tightened to 5 Nm. These plates were then inserted between two metallic plates maintained at 70 °C thanks to a water circulation loop.

Before the performance test, the MEA were first subjected to a conditioning and break-in stage consisting in:

- A 40 min temperature rise from 40 °C to 70 °C (each of the 10 °C steps being held 10 min) at Open Circuit Voltage (OCV), the anode and the cathode being both fed with 10 slph of nitrogen. Hydrogen is then introduced in the anode compartment (10 slph, 10 min) followed by air at the cathode (10 slph of air, 10 min).
- Two hours of constant voltage operation according to the following sequence: 0.6 V (45 s), open circuit (30 s) and 0.3 V (60 s).
- One-hour operation at a constant current density of 0.5 A/cm^2.

The gas supply during the constant voltage and constant current operation stages was identical to that of the performance test, i.e. pure hydrogen and air, both at 60% RH and atmospheric pressure, with stoichiometries equal to 1.5 and 4 at the anode and cathode, respectively.

The performance test consisted in repeating five time the following sequence:

- Measurement of the impedance spectra at 0.5 A/cm^2, with a frequency ranging between 0.02 Hz and 10 kHz. We usually choose 0.5 A/cm^2 to perform characterization test after accelerated stress test protocols because aged materials may not be able to operate properly at higher current density. In most of the cases, 0.5 A/cm^2 is sufficient to monitor the evolution of the fuel cell main impedance parameters [37–39].
- Measurement of the polarization curve. The fuel cell voltage was measured once by increasing the current density, then by decreasing the current density. The average voltage values were retained.
- Then the cathode compartment was flushed with nitrogen and the hydrogen permeation current (at 0.5 V) was measured. The cathode ElectroChemical Surface Area (ECSA) was also assessed by cycling the potential between 0.1 and 0.7 V at a sweep rate of 50 mV/s.
- Finally, the FC was operated 2 h at a constant current density of 0.5 A/cm^2.

This sequence was repeated five time to detect any possible malfunction and only the fifth measurement was considered for the submitted data. Note that with each MEA, the performance test was always repeated a second time after swapping the air and hydrogen flows, i.e. each electrode was used as an anode and a cathode.

3. Results and discussions

3.1. Effects of Fenton's reagents concentration on PFSA membranes

Fenton's reaction is a widely used accelerated chemical degradation test for PFSA membranes since it enables to reproduce the radicals environment observed during fuel cell operation. However, the literature shows a large variety of hydrogen peroxide (3–30%) and catalyst concentrations (3–6000 ppm). In addition, the protocols and/or operating conditions may not be precisely described, which can make difficult the comparison between different studies [8,11,25,32,33,40–48]. Recently, Frensch et al. [29] investigated the effect of Fenton's reagents concentration on chemical degradation of first generation Nafion® N115 membranes. The authors highlighted the dependence of the fluoride emissions on iron and hydrogen peroxide concentrations. In the present study, since we investigate second generation Nafion® membranes, it was necessary to conduct a similar approach on both NR211 and XL membranes by varying reagents concentration, as reported in Table 1.

The impact of Fenton's reagents on PFSA membranes is usually analyzed through the concentration of the degradation products; this approach can also be carried out by collecting water produced during fuel cell operation [11,12]. Fluoride ions, coming from the production of hydrofluoric acid (HF), are the best-known degradation products and the most commonly monitored [25,32,42–44,46], the results being often expressed in term of fluoride emission rate (FER). As a first step, NR211 and XL membranes are soaked in a 3 vol% hydrogen peroxide solution to establish a reference of degradation rate in the absence of iron ions. A non-negligible fluoride emission rate of 11 $\mu g/g_{Nafion}/h$ for both membranes is measured. In the case of Fenton's solution, the FER reveals a high dependence on reagents concentration (Fig. 3), as it significantly increases with the hydrogen peroxide concentration, regardless of ferrous ion concentration. However, increasing the ferrous ion concentration leads to a higher FER with the 20 vol% H_2O_2 solution only. Indeed, the fluoride emission rate is divided by 27 in the case of NR211 and divided by 9 in the case of XL when the ferrous ion concentration is increased from 1 ppm to 44 ppm, while keeping the H_2O_2 concentration constant (0.2 vol%). A high amount of ferrous ions in the solution does not increase the efficiency of the Fenton's reaction [49,50], probably because of parasitic reactions such as the oxidation of iron (II) by the hydroxyl radical ($HO^{\bullet}$):

$$Fe^{2+} + HO^{\bullet} \rightarrow Fe^{3+} + HO^{-}$$

Table 1
Experimental matrix for the *ex-situ* Fenton test.

Experiment #	Fe^{2+} concentration (ppm)	H_2O_2 concentration (vol%)
1	44	0.2
2	44	3
3	44	20
4	1	0.2
5	1	3
6	4	20

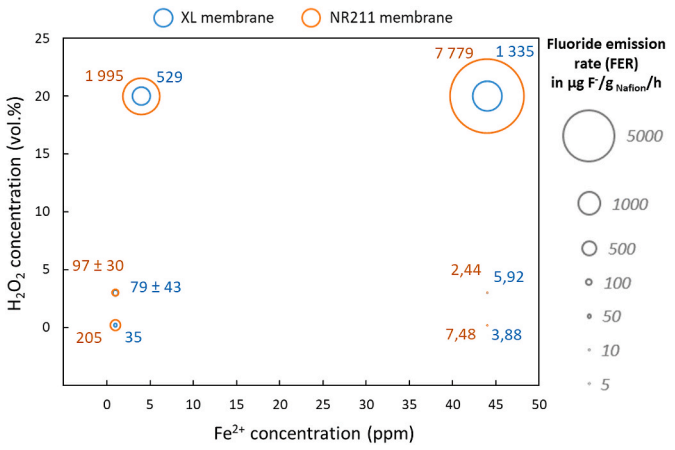

Fig. 3. Fluoride emission rates for Nafion® XL (in blue circle) & NR211 (in orange circle) membrane samples as a function of Fenton's reagents concentration. Reproducibility tests have been performed in the conditions that were chosen for combined chemical and mechanical stress test: 1 ppm Fe^{2+} and 3 v% H_2O_2. (For interpretation of the references to colour in this figure legend, the reader is referred to the Web version of this article.)

In addition to the consumption of hydroxyl radicals by such reactions, the low reaction rate of iron (II) regeneration limits the oxidizing power of the Fenton's reaction and consequently the membrane degradation. The use of a small amount of Fe^{2+} is thus required to efficiently catalyze the decomposition reaction of H_2O_2 in free radicals and ensure significant membrane degradation.

The stability of Nafion® membranes against hydrogen peroxide and Fenton's reagents has already been discussed in the literature by Kinumoto et al. [33]. Their work demonstrated that the presence of ferrous ion as counter ions enhanced significantly the decomposition rate of Nafion® membranes in comparison with protonated ones. These results support the assumption already presented in the literature that H_2O_2 acts as a necessary precursor to induce chemical degradation while ferrous ions act as a catalyst [29,51]. Interestingly, NR211 membranes always seem more affected than XL membranes, with FER 2 to 8 times higher.

Experiment #3 (Table 1), performed with high concentrations of both iron and hydrogen peroxide, leads to the most significant chemical degradation with a FER of 7.8 mg/g_{Nafion}/h for NR211 and 1.3 mg/g_{Nafion}/h for XL. On top of that, this experiment lasted only 3 min instead of 24 h in all the other cases and it was not possible to reach 80 °C. Indeed, Fenton's reaction being exothermic, the bubbling of the solution that occurred when the membrane is immersed becomes impossible to control when the temperature exceeds 40 °C.

The morphology of PFSA membranes can also be strongly affected by Fenton's reagents concentration and more particularly by high hydrogen peroxide concentration (around 20–30 vol%) [32,46]. For instance, Mu et al. [32] showed that a high concentration of H_2O_2 – with and without ferrous ions – entails the appearance of numerous cracks and holes. In our case, the naked eye examination of aged membranes confirms these morphological evolutions: many bubbles appear on the whole surface with both XL and NR211 membranes when the H_2O_2 concentrations is the highest (20 vol%). Fig. 4.a and **4.b** show pictures of pristine and aged XL and NR211 membranes for various Fenton's reagents concentration.

Furthermore, morphology evolutions differ significantly between the two membranes: bubbles with various diameters (from micrometers to millimeters) appear on the Nafion® XL surface while tiny bubbles in the micrometer range appear on NR211 when the reaction is conducted with 20 vol% H_2O_2 concentration (Fig. 5.b and **5.d**).

Many publications report morphological changes at the surface and in the thickness of the membrane when exposed to Fenton's solution with high H_2O_2 concentration [32,41,46,47,52–54]. More particularly,

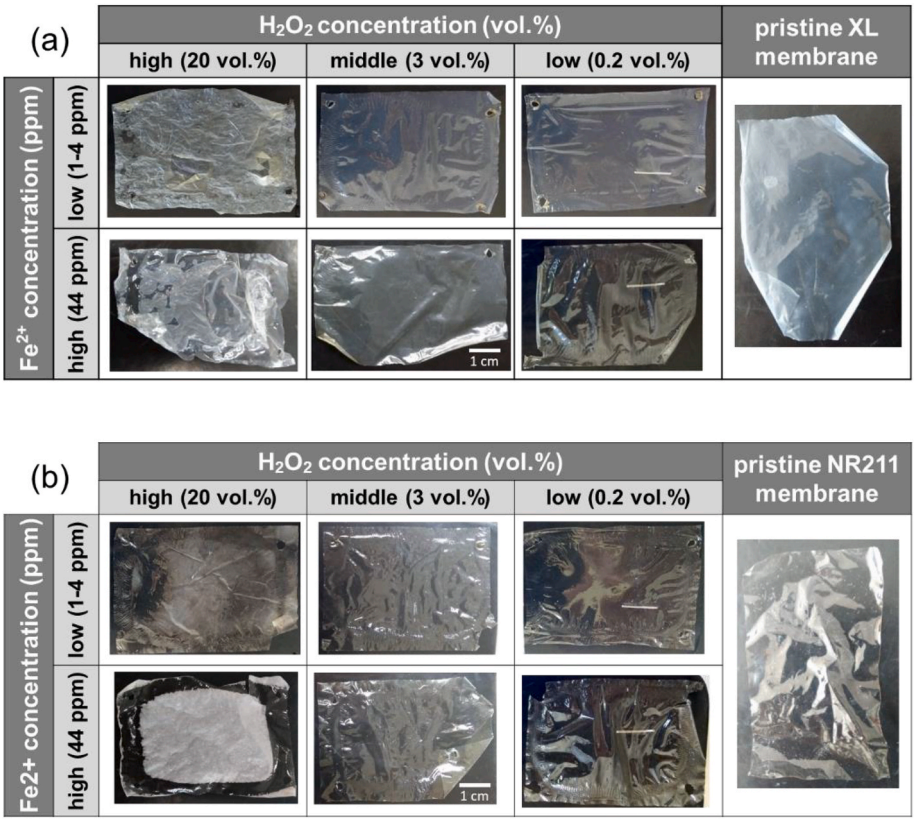

Fig. 4. Comparison of (a) XL and (b) NR211 macroscopic morphologies after exposure to the different Fenton's reagents concentrations.

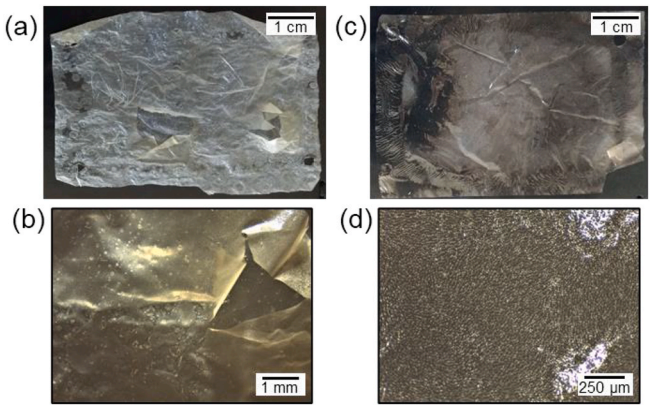

Fig. 5. Macroscopic changes after experiment #6 conducted with a high H_2O_2 concentration (20 vol%) and low Fe^{2+} concentration (4 ppm) for Nafion® XL, (a) without magnification and (b) with 8× magnification, as well as with Nafion® NR211, (c) without magnification and (d) with 35× magnification.

SEM images of the surface and cross-section of unreinforced Nafion® membranes revealed the presence of severe damages after Fenton's reagents treatment with the appearance of many bubbles, bumps and tears evolving into cracks and pinholes, up to the rupture of the membrane into two pieces or more. In conclusion, Fenton's reaction involving high H_2O_2 concentration entails an important chemical degradation of PFSA membranes but also significant morphological changes. Nevertheless, it is important to note that to the best of our knowledge, such morphological changes have not been observed – or at least reported – in fuel cells. Indeed, the consequences of membrane degradation during fuel cell operation are described as a membrane thinning resulting from chemical attacks of the polymer, as well as pinholes/cracks formation and propagation due to the mechanical constraints exerted by the flow field plates [6,7,10,11]. Furthermore, the H_2O_2 concentration in a fuel cell is estimated to be between 0.1 and 1.6 mmol L^{-1}, depending on the membrane thickness and on the side where it is formed (anode or cathode) [55–57]. The concentration used here – and in similar studies – to accelerate the degradation rate (i.e. 6.5 mol L^{-1} or 20 vol%) is therefore 3 to 4 orders of magnitude higher. And it must be kept in mind that the morphological changes observed in this case could imply different degradation mechanisms or pathways than those involved during fuel cell operation. In these regards, high H_2O_2 concentrations cannot be considered as the most adapted or representative. Consequently, with the objective to accelerate chemical degradation and thus fluoride emission rates (Fig. 3) without inducing significant morphological changes (Fig. 4), we chose to use 1 ppm of Fe^{2+} and 3 v% H_2O_2 in the rest of the study. Reproducibility tests have been performed in these "optimal" conditions, experiment #5 (Table 1) being repeated three times.

Table 2
Permeation current and high frequency resistance of aged Nafion® XL and Nafion® NR211 membranes for tests coupling 5 MPa compressive stress & H_2O_2 exposure (aging test #1) or Fenton's reagents exposure (aging test #2). Fourteen measurements of pristine XL membrane samples were carried out to control the repeatability of the measurements and of the MEA making process. In the other cases, tests were always repeated a second time after swapping the air and hydrogen flows, each electrode being used as an anode and a cathode, as mentioned in the end of section 2.4, and the results were averaged (the dispersion was negligible).

	Pristine membrane		Aging Test #1		Aging Test #2	
	XL	NR211	XL	NR211	XL	NR211
Permeation current (mA. cm^{-2})	1.01–2.58	1.30	0.86	4.50	1.03	2.58
High Frequency Resistance ($\Omega.cm^{-2}$)	0.071–0.086	0.066	0.105	0.073	0.106	0.072
Open Circuit Voltage (V)	0.904–0.930	0.921	0.920	0.878	0.904	0.894

3.2. *Impact of combined mechanical and chemical stress on PFSA membranes structure and properties*

The second step of our work was to generate a mechanical fatigue in a membrane exposed to an aggressive chemical environment in order to study the effects of the coupling. A custom-made device presented on Fig. 2 was designed for this purpose. A preliminary experiment was carried out in order to evaluate the endurance of the membranes under mechanical stress only: NR211 and XL samples were compressed at 5 MPa and 0.1 Hz while the compression cell was fed with a continuous flow of distilled water for 20 h. At the end of the test, naked eye observations show that XL and NR211 membranes seem to withstand rather well this treatment. Although plastic deformations occur – the location of the serpentine channel ribs could easily be seen at the membranes surface – no cracks or holes are visible. Moreover, and as expected, no fluoride ions are detected after 20 h meaning that no chemical degradation occurred.

The second test consisted in applying a cyclic compressive stress

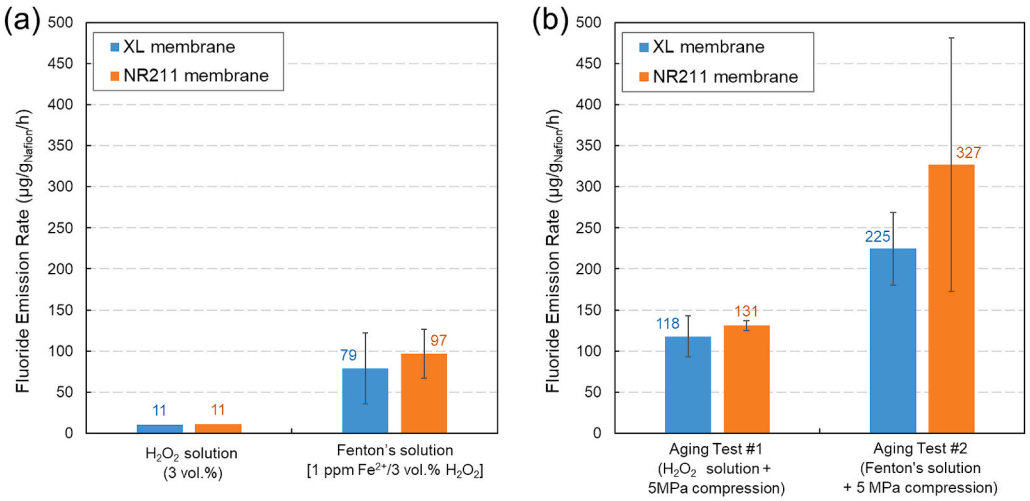

Fig. 6. Fluoride Emission Rates (FER) of Nafion® XL and NR211 membranes under (a) chemical or (b) both chemical and mechanical stressors. Experiments lasted 24 h when chemical stress only is applied and 8 h with combined chemical and mechanical stress.

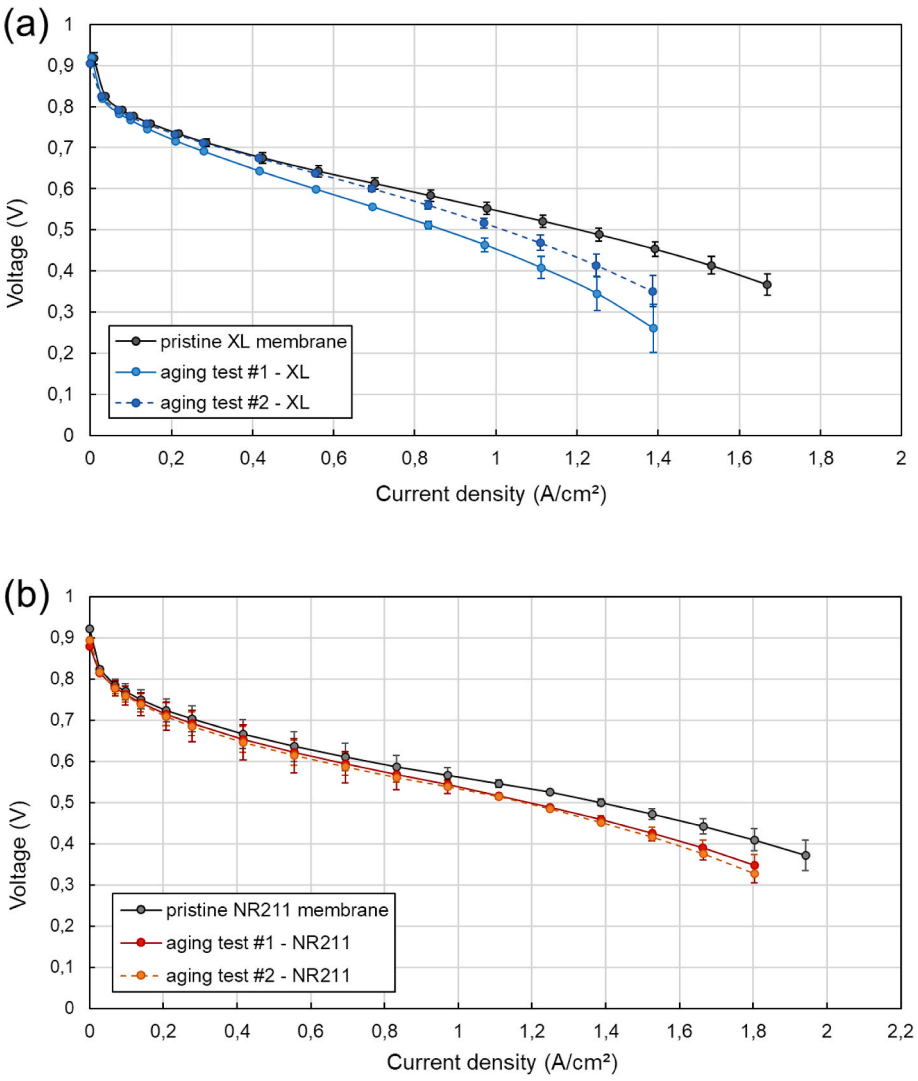

Fig. 7. Polarization curves in single cell with MEA made with (a) Nafion® XL and (b) Nafion® NR211 membranes. The cell was operated at 70 °C and supplied with pure hydrogen and air, both at 60% RH and atmospheric pressure. The gas stoichiometries were equal to 1.5 and 4 at the anode and cathode, respectively.

combined with the circulation of degrading solutions for 8 h. A first experiment was performed with hydrogen peroxide – without ferrous ions – to simulate moderately aggressive conditions. Another test was then performed with a Fenton's solution at the optimal concentration of reagents determined in section 3.1. Pristine membrane samples were used in each case. Fig. 6 compares the results obtained with and without mechanical stress in the different cases.

The fluoride emission rates measured for the different membrane degradation protocols vary considerably and follow a similar trend for both membranes. As seen in section 3.1, the degradation rate is significantly higher when the membranes are exposed to Fenton's reagents instead of hydrogen peroxide only. Adding a cyclic compressive stress does not modify this feature. Furthermore, the application of a cyclic compression seems to accelerate the chemical decomposition of the membrane: the combination of a 5 MPa sinusoidal constraint and 3 vol% H_2O_2 exposure (aging test #1) leads to fluoride emission rates about 10 and 12 times higher for XL and NR211, respectively, than in the case of chemical degradation (H_2O_2 solution) only. These results are similar to those obtained by Kusoglu et al. in the case of a static normal stress [25]. Moreover, the membrane degradation obtained by coupling mechanical fatigue and H_2O_2 exposure is more significant than that observed with Fenton's reagents exposure only.

When the cyclic compression (5 MPa) is combined with the exposure to the Fenton's reagents (aging test #2), the degradation rate increases: the fluoride emission rate reaches 225 $\mu g/g_{Nafion}/h$ for XL and 327 $\mu g/g_{Nafion}/h$ for NR211, which is about 3 times higher than that observed for exposure to the Fenton's reagents only. Interestingly, the degradation rate stays higher with NR211 than with XL100, but the values are more dispersed.

Finally, it must be mentioned that practical issues made it difficult to perform chemical degradation tests and combined chemical and mechanical degradation tests with similar durations. Furthermore, the membrane samples submitted to the combined stresses are in contact with a flowing – and constantly renewed – Fenton's solution. This may impact some of the results of this comparison study and further analyses will be performed to account for that difference.

To evaluate their functional properties and detect eventual hydrogen leaks, aged membranes were then used to make MEAs and tested in a single cell. The hydrogen crossover current was measured for both XL and NR211 membranes after the aging test #1 and #2 of Fig. 6 to ensure that no cracks or pinholes appeared. Moreover, polarization curves were also measured to confirm that the samples remained functional and possibly assess the impact of aging on cell performances. The permeation currents and high frequency resistances are reported in Table 2. No significant permeation current is measured for XL membranes, indicating that they withstand rather well the combined aging in both cases.

However, some localized bubbles were visible to the naked eye at the membrane surface after aging test #2. Conversely, NR211 membranes present no sign of degradation by macroscopic observations to the naked eye and using a stereo microscope, but a slight increase of the permeation current is observed after both aging tests. This may be the consequence of a membrane thinning or of microcracks that appeared through the membranes. Although the values we measured are not characteristic of critical membrane failure, they remain significant. Wang et al. [52] for instance obtained a permeation current of 7.04 mA/cm^2 after 24 h of Fenton's reagents exposure – with high H_2O_2 concentration (30 vol%) – and interpreted this as a degradation of the membrane (Nafion® 111), possibly because of the appearance of bubbles through its thickness. Furthermore, our experience of hydrogen permeation current monitoring during fuel cell accelerated stress tests show that such trends are often a good indication of imminent membrane failure.

The polarization curves measured with pristine and aged XL and NR211 membranes are shown in Fig. 7.a and **7.b**. The fuel cell performances of the aged XL membranes are lower than those obtained with the pristine ones: a slight increase of the resistive losses is observed, more particularly with the sample submitted to a H_2O_2 solution coupled with cyclic compression. This trend is not observed in the case of aged NR211 membranes for which no significant change of the polarization curve is perceptible except for a slight decrease of the open circuit voltage (see also Table 2), which can be explained by the increase of the hydrogen permeation current discussed above. This difference in behavior is also consistent with the values of the high frequency resistances, which showed no significant change with NR211 but increased slightly for the XL samples (Table 2). Furthermore, the membranes exposed only to Fenton's solution with the optimal concentration of reagents (*i.e.* without mechanical stress) for 24 h were also tested in single cell. No significant change of the polarization curves and no permeation currents are observed for both membranes suggesting that, under these conditions, the Fenton reaction had no impact on the membrane integrity or on the performance of the fuel cell. Finally, it is important to keep in mind that the increase of the resistive losses reported in Table 2 was to some extent linked to the plastic deformation of the membranes surface, which did not make it possible to assess properly their functional properties because of the poor quality of the interface with the electrodes. Nevertheless, the shape of the polarization curves confirms the absence of critical membrane failure.

4. Conclusions and perspectives

4.1. Effects of Fenton's reagents concentration on PFSA membranes

Our results highlight a high dependence of the membrane degradation on the Fenton's reagent concentrations, both from chemical and morphological points of view. The use of a small amount of Fe^{2+} is required to catalyze efficiently the decomposition reaction of H_2O_2 in free radicals and to ensure a significant membrane degradation. On the other hand, H_2O_2 concentrations must also be kept rather low (i.e. 3 vol % in our case) so that the degradation mechanisms (or pathways) can be considered as representative of those occurring during fuel cell operation, this because the H_2O_2 concentration in a fuel cell is most probably several orders of magnitude lower than that used for Fenton's reaction. Keeping the H_2O_2 concentration low makes it possible to avoid dramatic morphological changes of Nafion that are not assumed to occur during fuel cell operation.

4.2. Impact of combined mechanical and chemical stress on PFSA membranes

The severe mechanical stress that was applied in this work does not overcome or dominate chemical degradations, with a response of the samples to chemical stress that does not seem to differ, at least qualitatively: the degradation rates remain more significant when the membranes are exposed to Fenton's reagents instead of hydrogen peroxide only, and we observed higher fluoride emission rates with NR211 than with Nafion XL. In addition, even though plastic deformations are observed on the membrane surface after the experiments, the samples remain fully functional when tested in fuel cells with only a slight decrease of the performance that can be attributed to the degradation of the membrane-electrodes interface. This is most probably linked to the plastic deformation of the membrane samples, which were in direct contact with the channel ribs in the compression cell.

The better behavior of XL membranes *vs.* NR211 is explained by the presence of the additional reinforcement layer which provides better mechanical strength and dimensional stability [31,58]. The improved durability of XL membranes was already discussed in the literature and could be due to higher strength and toughness as well as a better resistance to creep and fatigue [59–63]. In this work, it was confirmed by constantly lower FER whatever the kind of aging test performed as well as the absence of significant modification in the hydrogen permeation current after combined mechanical and chemical accelerated stress tests, contrary to NR211 membranes.

4.3. Perspectives

The development of accelerated tests combining chemical and mechanical stresses is a necessary step to quickly assess the durability of membranes [30,31] and gain a deeper understanding of their degradation mechanisms. Nevertheless, the device that was designed for this work opens up various possibilities and supplementary works will be necessary to optimize the conditions in which such accelerated tests are performed. As a starting point, using strictly identical conditions regarding chemical degradation with and without a mechanical stress is required to conclude definitely on the effect of mechanical fatigue. In addition, the use of Gas Diffusion Layers (GDL) between the membrane and the flow field plates of the compression cell would probably better mimic the mechanical constraint encountered by the membranes during fuel cell operation and make it possible to better understand the impact of plastic deformation. Gas diffusion layers could also improve the distribution of the Fenton's solution at the surface of the membrane.

CRediT authorship contribution statement

Mylène Robert: Conceptualization, Methodology, Validation, Investigation, Data curation, Visualization, Writing - original draft, Writing - review & editing. **Jean-Christophe Perrin:** Conceptualization, Methodology, Supervision, Writing - original draft, Writing - review & editing. **Kévin Mozet:** Methodology, Visualization. **Meriem Daoudi:** Validation, Investigation. **Jérôme Dillet:** Conceptualization, Methodology, Software. **Jean-Yves Morel:** Conceptualization. **Stéphane André:** Conceptualization, Methodology. **Olivier Lottin:** Project administration, Conceptualization, Methodology, Writing - original draft, Writing - review & editing.

Declaration of competing interest

The authors declare that they have no known competing financial interests or personal relationships that could have appeared to influence the work reported in this paper.

References

[1] R. Borup, J. Meyers, B. Pivovar, Y.S. Kim, R. Mukundan, N. Garland, D. Myers, M. Wilson, F. Garzon, D. Wood, P. Zelenay, K. More, K. Stroh, T. Zawodzinski, J. Boncella, J.E. McGrath, M. Inaba, K. Miyatake, M. Hori, K. Ota, Z. Ogumi, S. Miyata, A. Nishikata, Z. Siroma, Y. Uchimoto, K. Yasuda, K. Kimijima, N. Iwashita, Scientific aspects of polymer electrolyte fuel cell durability and degradation, Chem. Rev. 107 (2007) 3904–3951, https://doi.org/10.1021/cr050182l.

[2] L. Dubau, L. Castanheira, F. Maillard, M. Chatenet, O. Lottin, G. Maranzana, J. Dillet, A. Lamibrac, J.-C. Perrin, E. Moukheiber, A. ElKaddouri, G. De Moor,

C. Bas, L. Flandin, N. Caque, A review of PEM fuel cell durability: materials degradation, local heterogeneities of aging and possible mitigation strategies, Wiley Interdiscip. Rev. Energy Environ. 3 (2014) 540–560, https://doi.org/10.1002/wene.113.
[3] J. Shan, R. Lin, S. Xia, D. Liu, Q. Zhang, Local resolved investigation of PEMFC performance degradation mechanism during dynamic driving cycle, Int. J. Hydrogen Energy 41 (2016) 4239–4250, https://doi.org/10.1016/j.ijhydene.2016.01.048.
[4] R. Lin, F. Xiong, W.C. Tang, L. Técher, J.M. Zhang, J.X. Ma, Investigation of dynamic driving cycle effect on the degradation of proton exchange membrane fuel cell by segmented cell technology, J. Power Sources 260 (2014) 150–158, https://doi.org/10.1016/j.jpowsour.2014.03.003.
[5] A. Kusoglu, A.Z. Weber, A mechanistic model for pinhole growth in fuel-cell membranes during cyclic loads, J. Electrochem. Soc. 161 (2014), https://doi.org/10.1149/2.036408jes. E3311–E3322.
[6] C.S. Gittleman, F.D. Coms, Y.-H. Lai, Chapter 2 - membrane durability: physical and chemical degradation, in: M.M. Mench, E.C. Kumbur, T.N. Veziroglu (Eds.), Polymer Electrolyte Fuel Cell Degradation, Academic Press, Boston, 2012, pp. 15–88, https://doi.org/10.1016/B978-0-12-386936-4.10002-8.
[7] G.D. Moor, C. Bas, N. Charvin, E. Moukheiber, F. Niepceron, N. Breilly, J. André, E. Rossinot, E. Claude, N.D. Albérola, L. Flandin, Understanding membrane failure in PEMFC: comparison of diagnostic tools at different observation scales, Fuel Cell. 12 (2012) 356–364, https://doi.org/10.1002/fuce.201100161.
[8] L. Ghassemzadeh, T.J. Peckham, T. Weissbach, X. Luo, S. Holdcroft, Selective formation of hydrogen and hydroxyl radicals by electron beam irradiation and their reactivity with perfluorosulfonated acid ionomer, J. Am. Chem. Soc. 135 (2013) 15923–15932, https://doi.org/10.1021/ja408032p.
[9] L. Ghassemzadeh, K.-D. Kreuer, J. Maier, K. Mueller, Chemical degradation of nation membranes under mimic fuel cell conditions as investigated by solid-state NMR spectroscopy, J. Phys. Chem. C 114 (2010) 14635–14645, https://doi.org/10.1021/jp102533v.
[10] S.-Y. Lee, E. Cho, J.-H. Lee, H.-J. Kim, T.-H. Lim, I.-H. Oh, J. Won, Effects of purging on the degradation of PEMFCs operating with repetitive on/off cycles, J. Electrochem. Soc. 154 (2007), https://doi.org/10.1149/1.2403083. B194–B200.
[11] J. Healy, C. Hayden, T. Xie, K. Olson, R. Waldo, A. Brundage, H. Gasteiger, J. Abbott, Aspects of the chemical degradation of PFSA ionomers used in PEM fuel cells, Fuel Cell. 5 (2005) 302–308, https://doi.org/10.1002/fuce.200400050.
[12] A.B. LaConti, M. Hamdan, R.C. McDonald, Mechanisms of membrane degradation, in: Handbook of Fuel Cells, John Wiley & Sons, Ltd, 2010, https://doi.org/10.1002/9780470974001.f303055.
[13] M. Zatoń, J. Rozière, D.J. Jones, Current understanding of chemical degradation mechanisms of perfluorosulfonic acid membranes and their mitigation strategies: a review, Sustain. Energy Fuels 1 (2017) 409–438, https://doi.org/10.1039/C7SE00038C.
[14] A. Collier, H. Wang, X. Zi Yuan, J. Zhang, D.P. Wilkinson, Degradation of polymer electrolyte membranes, Int. J. Hydrogen Energy 31 (2006) 1838–1854, https://doi.org/10.1016/j.ijhydene.2006.05.006.
[15] V.O. Mittal, H.R. Kunz, J.M. Fenton, Membrane degradation mechanisms in PEMFCs, J. Electrochem. Soc. 154 (2007), https://doi.org/10.1149/1.2734869. B652–B656.
[16] Nafion-XL-properties.pdf (n.d.), http://www.fuelcellsetc.com/store/DS/Nafion-XL-properties.pdf. (Accessed 29 May 2018).
[17] S. Shi, A.Z. Weber, A. Kusoglu, Structure/property relationship of Nafion XL composite membranes, J. Membr. Sci. 516 (2016) 123–134, https://doi.org/10.1016/j.memsci.2016.06.004.
[18] E. Moukheiber, G. De Moor, L. Flandin, C. Bas, Investigation of ionomer structure through its dependence on ion exchange capacity (IEC), J. Membr. Sci. 389 (2012) 294–304, https://doi.org/10.1016/j.memsci.2011.10.041.
[19] V. Prabhakaran, C.G. Arges, V. Ramani, Investigation of polymer electrolyte membrane chemical degradation and degradation mitigation using in situ fluorescence spectroscopy, Proc. Natl. Acad. Sci. U.S.A. 109 (2012) 1029–1034, https://doi.org/10.1073/pnas.1114672109.
[20] S.M. Stewart, D. Spernjak, R. Borup, A. Datye, F. Garzon, Cerium migration through hydrogen fuel cells during accelerated stress testing, ECS Electrochem. Lett. 3 (2014), https://doi.org/10.1149/2.008404eel. F19–F22.
[21] A.M. Baker, R. Mukundan, D. Spernjak, E.J. Judge, S.G. Advani, A.K. Prasad, R. L. Borup, Cerium migration during PEM fuel cell accelerated stress testing, J. Electrochem. Soc. 163 (2016), https://doi.org/10.1149/2.0181609jes. F1023–F1031.
[22] G. De Moor, C. Bas, N. Charvin, J. Dillet, G. Maranzana, O. Lottin, N. Caque, E. Rossinot, L. Flandin, Perfluorosulfonic acid membrane degradation in the hydrogen inlet region: a macroscopic approach, Int. J. Hydrogen Energy 41 (2016) 483–496, https://doi.org/10.1016/j.ijhydene.2015.10.066.
[23] M. Robert, A. El Kaddouri, J.-C. Perrin, S. Leclerc, O. Lottin, Towards a NMR-based method for characterizing the degradation of nafion XL membranes for PEMFC, J. Electrochem. Soc. 165 (2018), https://doi.org/10.1149/2.0231806jes. F3209–F3216.
[24] W. Yoon, X. Huang, Acceleration of chemical degradation of perfluorosulfonic acid ionomer membrane by mechanical stress: experimental evidence, ECS Trans 33 (2010) 907–911, https://doi.org/10.1149/1.3484584.
[25] A. Kusoglu, M. Calabrese, A.Z. Weber, Effect of mechanical compression on chemical degradation of nafion membranes, ECS Electrochem. Lett. 3 (2014) F33–F36, https://doi.org/10.1149/2.008405eel.
[26] S. velan Venkatesan, C. Lim, S. Holdcroft, E. Kjeang, Progression in the morphology of fuel cell membranes upon conjoint chemical and mechanical degradation, J. Electrochem. Soc. 163 (2016) F637–F643, https://doi.org/10.1149/2.0671607jes.
[27] V.M. Ehlinger, A. Kusoglu, A.Z. Weber, Modeling coupled durability and performance in polymer-electrolyte fuel cells: membrane effects, J. Electrochem. Soc. 166 (2019), https://doi.org/10.1149/2.0281907jes. F3255–F3267.
[28] L. Lin, M. Danilczuk, S. Schlick, Electron spin resonance study of chemical reactions and crossover processes in a fuel cell: effect of membrane thickness, J. Power Sources 233 (2013) 98–103, https://doi.org/10.1016/j.jpowsour.2013.01.117.
[29] S.H. Frensch, G. Serre, F. Fouda-Onana, H.C. Jensen, M.L. Christensen, S.S. Araya, S.K. Kær, Impact of iron and hydrogen peroxide on membrane degradation for polymer electrolyte membrane water electrolysis: computational and experimental investigation on fluoride emission, J. Power Sources 420 (2019) 54–62, https://doi.org/10.1016/j.jpowsour.2019.02.076.
[30] C. Lim, L. Ghassemzadeh, F. Van Hove, M. Lauritzen, J. Kolodziej, G.G. Wang, S. Holdcroft, E. Kjeang, Membrane degradation during combined chemical and mechanical accelerated stress testing of polymer electrolyte fuel cells, J. Power Sources 257 (2014) 102–110, https://doi.org/10.1016/j.jpowsour.2014.01.106.
[31] R. Mukundan, A.M. Baker, A. Kusoglu, P. Beattie, S. Knights, A.Z. Weber, R. L. Borup, Membrane accelerated stress test development for polymer electrolyte fuel cell durability validated using field and drive cycle testing, J. Electrochem. Soc. 165 (2018) F3085–F3093, https://doi.org/10.1149/2.0101806jes.
[32] S. Mu, C. Xu, Q. Yuan, Y. Gao, F. Xu, P. Zhao, Degradation behaviors of perfluorosulfonic acid polymer electrolyte membranes for polymer electrolyte membrane fuel cells under varied acceleration conditions, J. Appl. Polym. Sci. 129 (2013) 1586–1592, https://doi.org/10.1002/app.38785.
[33] T. Kinumoto, M. Inaba, Y. Nakayama, K. Ogata, R. Umebayashi, A. Tasaka, Y. Iriyama, T. Abe, Z. Ogumi, Durability of perfluorinated ionomer membrane against hydrogen peroxide, J. Power Sources 158 (2006) 1222–1228, https://doi.org/10.1016/j.jpowsour.2005.10.043.
[34] W. Grot, 9 - experimental methods, in: Fluorinated Ionomers, second ed., William Andrew Publishing, 2011, pp. 211–233, https://doi.org/10.1016/B978-1-4377-4457-6.10009-3.
[35] F. Xu, C. Innocent, B. Bonnet, D.J. Jones, J. Roziere, Chemical modification of perfluorosulfonated membranes with pyrrole for fuel cell application: preparation, characterisation and methanol transport, Fuel Cell. 5 (2005) 398–405, https://doi.org/10.1002/fuce.200400077.
[36] H.J.H. Fenton, LXXIII.—oxidation of tartaric acid in presence of iron, J. Chem. Soc. Trans. 65 (1894) 899–910, https://doi.org/10.1039/CT8946500899.
[37] S. Abbou, J. Dillet, D. Spernjak, R. Mukundan, J.D. Fairweather, R.L. Borup, G. Maranzana, S. Didierjean, O. Lottin, Time evolution of local potentials during PEM fuel cell operation with dead-ended anode, ECS Trans 58 (2013) 1631, https://doi.org/10.1149/05801.1631ecst.
[38] S. Abbou, J. Dillet, D. Spernjak, R. Mukundan, R.L. Borup, G. Maranzana, O. Lottin, High potential excursions during PEM fuel cell operation with dead-ended anode, J. Electrochem. Soc. 162 (2015), https://doi.org/10.1149/2.0511510jes. F1212.
[39] S. Abbou, J. Dillet, G. Maranzana, S. Didierjean, O. Lottin, Local potential evolutions during proton exchange membrane fuel cell operation with dead-ended anode – Part II: aging mitigation strategies based on water management and nitrogen crossover, J. Power Sources 340 (2017) 419–427, https://doi.org/10.1016/j.jpowsour.2016.10.045.
[40] D.E. Curtin, R.D. Lousenberg, T.J. Henry, P.C. Tangeman, M.E. Tisack, Advanced materials for improved PEMFC performance and life, J. Power Sources 131 (2004) 41–48, https://doi.org/10.1016/j.jpowsour.2004.01.023.
[41] H. Tang, S. Peikang, S.P. Jiang, F. Wang, M. Pan, A degradation study of Nafion proton exchange membrane of PEM fuel cells, J. Power Sources 170 (2007) 85–92, https://doi.org/10.1016/j.jpowsour.2007.03.061.
[42] C. Chen, G. Levitin, D.W. Hess, T.F. Fuller, XPS investigation of Nafion® membrane degradation, J. Power Sources 169 (2007) 288–295, https://doi.org/10.1016/j.jpowsour.2007.03.037.
[43] L. Merlo, A. Ghielmi, L. Cirillo, M. Gebert, V. Arcella, Resistance to peroxide degradation of Hyflon® Ion membranes, J. Power Sources 171 (2007) 140–147, https://doi.org/10.1016/j.jpowsour.2006.11.012.
[44] L. Ghassemzadeh, K.D. Kreuer, J. Maier, K. Mueller, Evaluating chemical degradation of proton conducting perfluorosulfonic acid ionomers in a Fenton test by solid-state F-19 NMR spectroscopy, J. Power Sources 196 (2011) 2490–2497, https://doi.org/10.1016/j.jpowsour.2010.11.053.
[45] X. Luo, L. Ghassemzadeh, S. Holdcroft, Effect of free radical-induced degradation on water permeation through PFSA ionomer membranes, Int. J. Hydrogen Energy 40 (2015) 16714–16723, https://doi.org/10.1016/j.ijhydene.2015.07.118.
[46] S. Kundu, L.C. Simon, M.W. Fowler, Comparison of two accelerated Nafion™ degradation experiments, Polym. Degrad. Stabil. 93 (2008) 214–224, https://doi.org/10.1016/j.polymdegradstab.2007.10.001.
[47] A.C. Fernandes, E.A. Ticianelli, A performance and degradation study of Nafion 212 membrane for proton exchange membrane fuel cells, J. Power Sources 193 (2009) 547–554, https://doi.org/10.1016/j.jpowsour.2009.04.038.
[48] V.A. Sethuraman, J.W. Weidner, A.T. Haug, L.V. Protsailo, Durability of perfluorosulfonic acid and hydrocarbon membranes: effect of humidity and temperature, J. Electrochem. Soc. 155 (2008), https://doi.org/10.1149/1.2806798. B119–B124.
[49] Z. Stuglik, Z. PawełZagórski, Pulse radiolysis of neutral iron(II) solutions: oxidation of ferrous ions by OH radicals, Radiat. Phys. Chem. 17 (1981) (1977) 229–233, https://doi.org/10.1016/0146-5724(81)90336-8.
[50] E. Brillas, I. Sirés, M.A. Oturan, Electro-fenton process and related electrochemical technologies based on Fenton's reaction chemistry, Chem. Rev. 109 (2009) 6570–6631, https://doi.org/10.1021/cr900136g.

[51] S. Hommura, K. Kawahara, T. Shimohira, Y. Teraoka, Development of a method for clarifying the perfluorosulfonated membrane degradation mechanism in a fuel cell environment, J. Electrochem. Soc. 155 (2008), https://doi.org/10.1149/1.2800171. A29–A33.
[52] F. Wang, H. Tang, M. Pan, D. Li, Ex situ investigation of the proton exchange membrane chemical decomposition, Int. J. Hydrogen Energy 33 (2008) 2283–2288, https://doi.org/10.1016/j.ijhydene.2008.01.052.
[53] X. Sun, S. Shi, Y. Fu, J. Chen, Q. Lin, J. Hu, C. Li, J. Li, X. Chen, Embrittlement induced fracture behavior and mechanisms of perfluorosulfonic-acid membranes after chemical degradation, J. Power Sources 453 (2020), 227893, https://doi.org/10.1016/j.jpowsour.2020.227893.
[54] K. Hongsirikarn, X. Mo, J.G. Goodwin, S. Creager, Effect of H2O2 on Nafion® properties and conductivity at fuel cell conditions, J. Power Sources 196 (2011) 3060–3072, https://doi.org/10.1016/j.jpowsour.2010.11.133.
[55] W. Liu, D. Zuckerbrod, In situ detection of hydrogen peroxide in PEM fuel cells, J. Electrochem. Soc. 152 (2005), A1165, https://doi.org/10.1149/1.1904988.
[56] C. Chen, T. Fuller, H2O2 formation under fuel-cell conditions, ECS Trans 11 (2007) 1127, https://doi.org/10.1149/1.2781025.
[57] A.A. Shah, T.R. Ralph, F.C. Walsh, Modeling and simulation of the degradation of perfluorinated ion-exchange membranes in PEM fuel cells, J. Electrochem. Soc. 156 (2009) B465, https://doi.org/10.1149/1.3077573.
[58] M.P. Rodgers, L.J. Bonville, R. Mukundan, R.L. Borup, R. Ahluwalia, P. Beattie, R. P. Brooker, N. Mohajeri, H.R. Kunz, D.K. Slattery, J.M. Fenton, Perfluorinated sulfonic acid membrane and membrane electrode assembly degradation correlating accelerated stress testing and lifetime testing, ECS Trans 58 (2013) 129–148, https://doi.org/10.1149/05801.0129ecst.
[59] Y. Tang, A. Kusoglu, A.M. Karlsson, M.H. Santare, S. Cleghorn, W.B. Johnson, Mechanical properties of a reinforced composite polymer electrolyte membrane and its simulated performance in PEM fuel cells, J. Power Sources 175 (2008) 817–825, https://doi.org/10.1016/j.jpowsour.2007.09.093.
[60] N.S. Khattra, Z. Lu, A.M. Karlsson, M.H. Santare, F.C. Busby, T. Schmiedel, Time-dependent mechanical response of a composite PFSA membrane, J. Power Sources 228 (2013) 256–269, https://doi.org/10.1016/j.jpowsour.2012.11.116.
[61] E. Moukheiber, C. Bas, L. Flandin, Understanding the formation of pinholes in PFSA membranes with the essential work of fracture (EWF), Int. J. Hydrogen Energy 39 (2014) 2717–2723, https://doi.org/10.1016/j.ijhydene.2013.03.031.
[62] Q. Lin, Z. Liu, L. Wang, X. Chen, S. Shi, Fracture property of Nafion XL composite membrane determined by R-curve method, J. Power Sources 398 (2018) 34–41, https://doi.org/10.1016/j.jpowsour.2018.07.052.
[63] Z. Zhang, S. Shi, Q. Lin, L. Wang, Z. Liu, P. Li, X. Chen, Exploring the role of reinforcement in controlling fatigue crack propagation behavior of perfluorosulfonic-acid membranes, Int. J. Hydrogen Energy 43 (2018) 6379–6389, https://doi.org/10.1016/j.ijhydene.2018.02.034.